ChemComm

COMMUNICATION

View Article Online
View Journal | View Issue

Published on 19 July 2016. Downloaded by FAC DE QUIMICA on 19/05/2017 20:49:15.

Cite this: *Chem. Commun.*, 2016, 52, 10273

Received 6th June 2016,
Accepted 19th July 2016

DOI: 10.1039/c6cc04734c

www.rsc.org/chemcomm

CO_2 capture enhancement in InOF-1 *via* the bottleneck effect of confined ethanol†

Ricardo A. Peralta,[a] Alberto Campos-Reales-Pineda,[a] Heriberto Pfeiffer,[a] J. Raziel Álvarez,[a] J. Antonio Zárate,[a] Jorge Balmaseda,[a] Eduardo González-Zamora,*[b] Ana Martínez,[a] Diego Martínez-Otero,[c] Vojtech Jancik*[c] and Ilich A. Ibarra*[a]

CO_2 capture of InOF-1 was enhanced 3.6-fold, at 1 bar and 30 °C, by confining EtOH within its pores. Direct visualisation by single crystal X-ray diffraction revealed that EtOH divides InOF-1 channels in wide sections separated by "bottlenecks" caused by EtOH molecules bonded to the μ_2-OH functional groups of InOF-1.

Global warming is one of the greatest threats to human civilisation. In particular, the increasing levels of anthropogenic carbon dioxide (CO_2) emissions from fossil fuel combustion[1] directly impact our environment causing the continuous rise of temperatures across the planet. Currently, many world leaders and governments are promoting the development of new technologies for efficient and effective CO_2 sequestration.[2] Porous metal–organic frameworks (MOFs) or porous coordination polymers (PCPs) are amongst the most promising candidates for CO_2 capture because their CO_2 sorption capacity is directly tuneable as a function of the topology and chemical composition of the micropores.[3] An emerging CO_2 capture technology is based on the preparation of hybrid adsorbent materials which can be synthesised by confining solvents inside porous solid supports.[4] It is believed that solvent confinement can promote gas solubility considerably over the corresponding macroscopic values and therefore CO_2 capture enhancement. In this regard, Bratko and Luzar[5] predicted a 15-fold increase in CO_2 sequestration when water was confined in a hydrophobic environment, which was confirmed by Llewellyn[6] who reported a 5-fold increase in CO_2 capture by confining water in MIL-100(Fe). Similarly, Walton *et al.*[7] demonstrated that small amounts of confined water enhance CO_2 capture in PCPs that incorporate –OH functional groups within the pores. However, to the best of our knowledge, confined alcohol has never been used to enhance CO_2 capture inside a PCP. To investigate this possibility, we have chosen a PCP material entitled InOF-1[8] composed of binuclear [$In_2(\mu_2$-OH)] building blocks bridged by $BPTC^{4-}$ ligands (H_4BPTC = biphenyl-3,3′,5,5′-tetracarboxylic acid) (Fig. S1, ESI†). Furthermore, InOF-1 shows a 3-D framework structure with channel openings of approximately 7.5 Å (considering the van der Waals radii of the surface atoms). It also represents an ideal system for the study of the effect of confined alcohol on CO_2 sequestration as the hydroxo (μ_2-OH) functional groups are located inside the channels and can play a fundamental role in the solvent confinement effect.

Herein, we report a 2.7-fold (kinetic experiment, 30 °C) or 3.6-fold (static experiment, 30 °C) increase in CO_2 capture at one bar of CO_2 upon filling 10% of the pore volume of InOF-1 by ethanol, together with the ethanol adsorption properties of InOF-1 and the direct visualisation of these ethanol molecules in ethanol saturated InOF-1 through single crystal X-ray diffraction experiments.

Dynamic and isothermal CO_2 experiments were carried out on InOF-1. First, an acetone-exchanged sample of InOF-1 was activated (see Experimental details and Fig. S2 and S3 in the ESI†) and a kinetic CO_2 uptake experiment (at 30 °C) showed a maximum CO_2 capture of 5.24 wt%, which was rapidly reached after only 5 min and remained constant until the end of the experiment (20 min, Fig. S4, InOF-1, ESI†). Later, an acetone-exchanged sample of InOF-1 was activated, cooled at 30 °C (under N_2) and 10% of the pore volume was filled with ethanol (EtOH) *via* a solvent wet impregnation method (see the Experimental details in the ESI† and ref. 9). Hereinafter, this sample will be referred to as impregnated InOF-1. The 10% EtOH loading is based on the investigation of confined H_2O in the micropores of MIL-53(Cr),[10] in which Paesani demonstrated using computational infrared spectroscopy that at low water loadings, these water molecules interact strongly with the hydroxo

[a] *Instituto de Investigaciones en Materiales, Universidad Nacional Autónoma de México, Circuito Exterior s/n, CU, Del. Coyoacán, 04510, Ciudad de México, Mexico. E-mail: argel@unam.mx; Fax: +52(55) 5622-4595*

[b] *Departamento de Química, Universidad Autónoma Metropolitana-Iztapalapa, San Rafael Atlixco 186, Col. Vicentina, Iztapalapa, C. P. 09340, Ciudad de México, Mexico. E-mail: egz@xanum.uam.mx*

[c] *Centro Conjunto de Investigación en Química Sustentable UAEM-UNAM, Carr. Toluca-Atlacomulco Km 14.5, Toluca, Estado de México 50200, Mexico. E-mail: vjancik@unam.mx*

† Electronic supplementary information (ESI) available: Crystal structure data, experimental, TGA data, PXRD data, CO_2 capture studies, solvent wet impregnation method, ethanol adsorption data, adsorption microcalorimetry for EtOH, Fowler–Guggenheim type adsorption isotherm (FGAI), computational model and CO_2 separation experiments. CCDC 1477458 and 1477459. For ESI and crystallographic data in CIF or other electronic format see DOI: 10.1039/c6cc04734c

Published on 19 July 2016. Downloaded by FAC DE QUIMICA on 19/05/2017 20:49:15.

(μ_2-OH) functional groups, *via* hydrogen bonding, which are located inside the pore walls of MIL-53(Cr).

Therefore, we hypothesised that at low EtOH loadings, the microporous channels of InOF-1 can accommodate very efficiently these EtOH molecules since the μ_2-OH functional groups act as a template to 'pin' them. Consequently, these confined EtOH molecules help to accommodate more efficiently CO_2 molecules and finally enhance the total CO_2 capture.[7] Then, a kinetic CO_2 experiment, at 30 °C, was performed on the impregnated InOF-1 sample (300 mg of an activated InOF-1 sample were carefully impregnated with 0.011 mL of EtOH, with the help of a micropipette). Remarkably, the maximum amount of CO_2 captured corresponded to 14.14 wt%, which was reached in approximately 5 min and it was constant until 20 min (Fig. S4a, impregnated InOF-1, ESI†). To evaluate the reproducibility of the sample impregnation, six different samples of InOF-1 were impregnated and kinetic CO_2 experiments were performed (Fig. S4b, average of 14.07 wt%, ESI†). It is worth mentioning that we carried out the impregnation of InOF-1 samples with anhydrous ethanol (<0.005% water) and ethanol (reagent alcohol, 95%) and there was no difference in the maximum amount of CO_2 captured. In addition, we also explored filling 8%, 12% and 15% of the pore volume of the material with EtOH to confirm that the best results were obtained by filling 10% of the pores with EtOH. Thus, an approximately 2.7-fold increase in the CO_2 capture (from 5.24 wt% to 14.14 wt%) was observed when the sample was impregnated with EtOH in comparison to the non-impregnated sample. Moreover, the 2.7-fold increase was reached at the same time (~5 min) as for the non-impregnated sample, which clearly indicates that CO_2 adsorption kinetics were highly improved due to the presence of EtOH.

With the goal of investigating more about our hypothesis of low EtOH loadings, in the micro-porous channels of InOF-1, the pore volume of the material was filled from 85% with EtOH (solvent wet impregnation method, see the ESI†). This sample is referred as saturated InOF-1 in this work. Then, a kinetic CO_2 experiment (at 30 °C) was carried out on this sample. Interestingly, the amount of CO_2 captured was equal to 0.2 wt% (Fig. S4, saturated InOF-1, ESI†). We then rationalised that when the pore volume of the material is filled with 85% of EtOH, the saturation of the micropores in InOF-1, with EtOH molecules, was completed and therefore, the inclusion of CO_2 molecules, into the micropores, was unfeasible. PXRD analysis (Fig. S5, ESI†) confirmed the retention of the crystallinity in all samples after each CO_2 capture experiment.

Pera-Titus and Farrusseng[9,11] demonstrated through static and isothermal H_2 adsorption experiments the enhancement of the H_2 uptake by confining solvents such as *n*-hexane or ethanol in different mesoporous materials. In particular, the porous coordination polymer MIL-101(Cr) showed an approximately 2-fold increase in the H_2 uptake (at 298 K and 30 bar) by confining *n*-hexane.[9] Thus, another way to confirm the enhanced CO_2 capture by confining ethanol is static and isothermal adsorption experiments as demonstrated by Farrusseng[9] for H_2 in the MIL-101(Cr) system. The total CO_2 uptake (see Experimental details in the ESI†) at 303 K and 16 bar (Fig. 1, InOF-1) was 15 mmol g^{-1} (66.0 wt%). At 1 bar and 303 K, the uptake was equal to 3.81 mmol g^{-1}, which is in good agreement with the previously reported value of 4.02 mmol g^{-1} at 1 bar and 296 K.[8] Later, an impregnated InOF-1 (10% EtOH, see the ESI†) exhibited a total CO_2 capture of 20.2 mmol g^{-1} (88.9 wt%) at 16 bar (Fig. 1, impregnated InOF-1). Remarkably, at only 1 bar and 30 °C, the CO_2 capture was equal to 13.7 mmol g^{-1} (60.3 wt%). Therefore, at 16 bar and 30 °C the CO_2 capture increased by approximately 1.3-fold when the sample was impregnated with EtOH (from 15 to 20.2 mmol g^{-1}) in comparison to the non-impregnated sample. Outstandingly, at 1 bar and 30 °C, the CO_2 capture was approximately 3.6-fold increased (from 3.8 to 13.7 mmol g^{-1}).

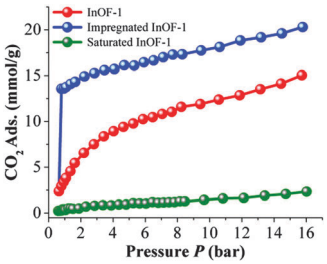

Fig. 1 Static CO_2 uptake experiments carried out from 0 to 16 bar at 30 °C on InOF-1 (red curve), impregnated InOF-1 (10% of the pore volume filled with EtOH, blue curve) and saturated InOF-1 (85% of the pore volume filled with EtOH, green curve).

Finally, the pore volume of an activated InOF-1 sample was filled from 85% with EtOH and the total uptake at 16 bar was approximately 2.3 mmol g^{-1} (10.1 wt%) and at 1 bar and 30 °C, the CO_2 capture was only 0.3 mmol g^{-1} (1.3 wt%), (Fig. 1, saturated InOF-1). This very low CO_2 uptake represents the adsorption on the surface of the microporous material rather than the adsorption inside the pores. As previously showed by kinetic CO_2 experiments, when the sample is impregnated from 85% with EtOH the saturation of the micropores in InOF-1 occurs and thus, there is no effective CO_2 capture. PXRD experiments demonstrated (Fig. S5, ESI†) the retention of the crystallinity in all samples.

Ethanol sorption experiments were performed on acetone-exchanged samples of InOF-1 at 20 and 30 °C, (see the ESI†). At 30 °C, ethanol underwent rapid uptake at low pressure, leading to saturation below $\%P/P_0$ = 10, indicative of favourable host–guest interactions, with a total uptake of 24.7 wt% (~12.6 molecules per unit cell). Minor hysteresis was observed (range from $\%P/P_0$ = 0 to 20) in the desorption phase (Fig. S6, open symbols, ESI†). This observed hysteresis is most likely due to the fact that ethanol molecules can form hydrogen bonds with the bridging hydroxo functional groups (μ_2-OH), within the pores, as we previously hypothesised.[12] The isosteric enthalpy of adsorption for EtOH (molar enthalpy of adsorption, ΔH) was experimentally measured by EtOH adsorption microcalorimetry (see Fig. S8 and S9, ESI,† ΔH = 45.04 kJ mol^{-1}) and also calculated by using the Fowler–Guggenheim Adsorption Isotherm (FGAI).[13] This methodology provided us with a very accurate fit for both experimental EtOH adsorption isotherms (ethanol at 20 and 30 °C, see the ESI† for fittings and mathematical treatment of equations) and the calculated molar enthalpy of

 This journal is © The Royal Society of Chemistry 2016

Published on 19 July 2016. Downloaded by FAC DE QUIMICA on 19/05/2017 20:49:15.

adsorption, at $\vartheta = 0$, was equal to $\Delta H = 44.61$ kJ mol^{-1} (Fig. S13, ESI†) which is in good agreement with the experimental value. This value is slightly higher than the molar enthalpy of vaporisation for ethanol[14] (42.32 kJ mol^{-1}). The proximity of both enthalpies for ethanol (vaporisation and adsorption), explains the shape of both adsorption isotherms: at 20 and 30 °C there is no inflexion point in the shape of the isotherms (Fig. S6 and S7, ESI†), suggesting only one domain of adsorption.[15] In addition, the enthalpy of adsorption for ethanol is in good agreement with PCP systems that exhibit bridging hydroxo functional groups (μ_2-OH) such as MIL-53(Cr).[16] Ethanol adsorption–desorption recyclability of InOF-1, was carried out, on the same sample, (Fig. S14 and S15, ESI†) with no apparent decrease in capacity (24.7 wt% at 30 °C) and adsorption kinetics over four cycles and showed a partial regeneration (retaining only 5 wt% of EtOH) of the material solely by evacuation for only 30 min without any thermal activation.

To establish the role of ethanol in the adsorption of CO_2 in the InOF-1 channels, we decided to determine the crystal structure of InOF-1 saturated completely with ethanol. To do so, the InOF-1 crystals were first rinsed with ethanol and dried to eliminate any trace of residual solvents that could interfere with the study. Despite the harsh treatment (170 °C and high vacuum), the inner crystalline structure of the crystals was retained, and it was possible to collect a full dataset and determine the crystal structure of the "empty" **InOF-1A** (Table S1, ESI†). Such dried crystals were soaked in anhydrous ethanol for two days, and another crystal was selected and measured under the same conditions (**InOF-1B**, Table S1, ESI†). In this case, it was possible to locate a highly disordered ethanol molecule hydrogen-bonded to the $In_2(\mu_2$-OH) group. It is noteworthy that the oxygen atom of the OH group is not accessible from inside of the channel, as it is located behind the proton and inside a "dent in the wall". Also, the position of the proton of the OH group was determined from the difference electron density map excluding its transfer to the ethanol molecule. The rest of the channels are filled with 7.25 amorphously frozen ethanol molecules as determined by the SQUEEZE routine.[17] Thus in total, the unit cell contains approximately 15.25 ethanol molecules. Remarkably, this number is only 2.6 molecules of ethanol per unit cell more than is adsorbed by the activated InOF-1 at 30 °C and an atmospheric pressure of ethanol vapour. This is a very consistent result since the single crystal X-ray diffraction experiment was carried out at 100 K (−173 °C) which is a much lower temperature than 30 °C and the crystals were taken directly from absolute ethanol. The high structural stability of the InOF-1 framework is also reflected in the practically identical bond lengths and angles in both crystal structures (Table S2, ESI†). The O···O distances between the OH group and the two ethanol positions in **InOF-1B** are 2.73 Å (71% occupancy) and 2.92 Å (29% occupancy) indicating a very strong hydrogen bond at the main position.

The structures of **InOF-1A** and **InOF-1B** were used to visualise the effect of the confined ethanol on the diameter and shape of the pore (Fig. 2) to try to explain the exceptional adsorption properties of the impregnated InOF-1. In **InOF-1A**, the channel is practically cylindrical with a diameter of 7.5 Å. The presence of one hydrogen bond linked ethanol molecule inside this channel has a dramatic effect on the free cross-section of the void in the

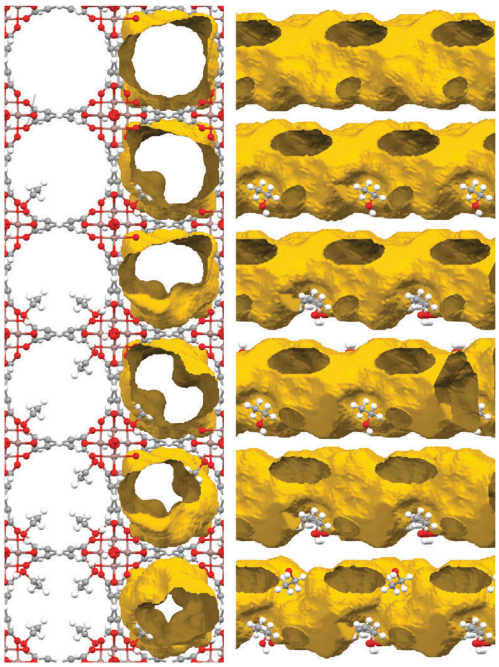

Fig. 2 Crystal structures of **InOF-1A** (top) and **InOF-1B** (bottom) and the effect of the amount of ethanol confined in the pores *via* the formation of a hydrogen bond to the $In_2(\mu_2$-OH) hydroxo groups on the pore diameter and shape. View along the crystallographic 001 direction with and without the channel surface (left) and along the 110 direction rotated additionally by 35° around 010 (right) to demonstrate the change from an almost cylindrical to a helicoidal shape.

place of the ethanol as it gets significantly reduced by the ethyl group pointing in the centre of the channel. As can be seen from Fig. 2, each subsequent molecule of ethanol not only diminishes further the free cross-section of the pore but also due to the symmetry of the network deforms the shape of the channel significantly. Thus, in **InOF-1B**, where all OH groups are bonded to ethanol molecules, the pore is helix-shaped with an approximate cross-section of the free space between 3.7 and 4.5 Å and pore volume of 945 Å^3 per unit cell (determined using a model without disorder). Thus, the kinetic diameter of CO_2 (3.3 Å)[18] practically inhibits the direct passage of the CO_2 molecules through the network and therefore results in a lower adsorption. This was demonstrated by the virtually zero adsorption of CO_2 on the 85% impregnated sample of InOF-1 (*vide supra*).

Furthermore, the pore volume of 1504 Å^3 in the unit cell of **InOF-1A** determined by crystallography can be converted to 0.39 cm^3 g^{-1} and is in excellent agreement with the BET studies indicating this volume to be 0.37 cm^3 g^{-1}. The loading of 10% of the pore volume with ethanol used in the adsorption studies means that if all ethanol molecules were adsorbed and uniformly distributed in the bulk material, there would be approximately 1.35 molecules of ethanol in the unit cell. It is safe to conclude that in this case all the ethanol would be involved in hydrogen bonds with the hydroxo bridges. These hydroxo bridges are all equivalent, as they are related by the 4_1 screw axis. This creates an interesting situation, as at even distribution, there would be two molecules of ethanol in each 37 Å of the length of the channel

Published on 19 July 2016. Downloaded by FAC DE QUIMICA on 19/05/2017 20:49:15.

dividing it efficiently into wide sections separated by a "bottleneck" caused by the bonded ethanol. As can be seen from Fig. 2, this "bottleneck" effect is not too big to inhibit the CO_2 molecules to pass this point, but will force them to "stop" or "slow down". This can be compared to a busy "multiline highway", where a quarter of the lines are suddenly closed by a roadblock and local "traffic jam" is created. In the impregnated InOF-1, this "traffic jam" would in the case of a uniform distribution of the ethanol molecules repeat approximately every 19 Å. This also explains why this effect cannot be replicated in materials with a smaller pore size but without confined solvent. In this case, the "blocked lines" are missing permanently. Another factor that probably helps to keep the CO_2 in the impregnated InOF-1 is the availability of a large number of free OH groups on the surface of the channels, which can bind the CO_2 molecules through the formation of $O{=}C{=}O(\delta^-)\cdots H(\delta^+)$ hydrogen bonds as previously demonstrated by Yang, in a material isostructural to InOF-1 labelled as NOTT-300.[19]

The CO_2–InOF-1 adsorbate–adsorbent system involves mainly three types of interactions: CO_2–CO_2 (similar to the bulk liquid), dispersion CO_2–InOF-1, and CO_2–quadrupole moment tensor with the electric field gradient of InOF-1.[20] When the system is free of EtOH molecules, the subsystem of CO_2 molecules can behave like an ideal gas since the channels of InOF-1 do not impose any steric hindrance and the experimental temperature (30 °C) and critical temperature of CO_2 (30.98 °C) are very close.[21] At 30 °C, the thermal energy ($\sim$2.5 kJ mol^{-1}) is enough to overcome potential barriers that are imposed by the weak adsorbate–adsorbent interactions to finally achieve a non-localised adsorption. Indeed, the entropy of the CO_2 subsystem is changed with the pre-adsorption of EtOH molecules. The bottlenecks created by these EtOH molecules, reduce the self-diffusion coefficient of CO_2 forcing CO_2 molecules to spend considerably more time around the bottlenecks under large steric constraints. These adsorbed ethanol molecules also impose steric restrictions on the CO_2 molecules that are adsorbed next to them. Ethanol and constrained CO_2 molecules affect the configuration of free CO_2 molecules, localised between bottlenecks and thus, the overall effect is a reduction in their molar volume and energy. This is clearly observed in the CO_2 adsorption isotherm slope of the impregnated InOF-1, (Fig. 1). Finally, the present study demonstrates that loading 10% of the pore volume with ethanol represents a perfect equilibrium, where the "bottleneck" effect is maximised, and there is no excessive saturation of the channels by ethanol, thus maximizing also the adsorption of CO_2.

Quantum chemical calculations (Molecular Electrostatic Potential, MEP) showed that a CO_2 molecule should bind to the OH group of an ethanol molecule which, in turn, is hydrogen-bonded to the μ_2-OH functional group of InOF-1 (see the ESI†, Fig. S18). Finally, CO_2 column separation studies (see the ESI†), demonstrated that impregnated InOF-1 showed a considerably higher affinity towards CO_2 compared to the fully activated InOF-1 material (see the ESI†).

CO_2 capture enhancement was successfully achieved by confinement of EtOH within the micropores of InOF-1. The direct visualisation of a very strong hydrogen bond between the OH group (μ_2-OH) and the EtOH molecule was possible by means of single crystal X-ray diffraction. These bonded EtOH molecules create a "bottleneck effect" which can accommodate CO_2 molecules more efficiently, by partially blocking the pores of InOF-1, resulting in a remarkably enhanced CO_2 capture.

The authors thank Dr A. Tejeda-Cruz (powder X-ray; IIM-UNAM), CONACyT (212318), PAPIIT UNAM (IN100415), Mexico for financial support. A. M. thanks NES supercomputer, (DGTIC-UNAM). E. G-Z. thanks CONACyT (236879), Mexico, for financial support. Thanks to U. Winnberg (ITAM) for scientific discussions. J. B. thanks the financial support of CIQA project 2016/6317. V. J. acknowledges the financial support of CONACyT (179348). We would also like to thank to Prof. K. Sumida (The University of Adelaide) for his encouragement.

Notes and references

1 S. Chu, *Science*, 2009, **325**, 1599.
2 (*a*) D. M. D'Alessandro, B. Smit and J. R. Long, *Angew. Chem., Int. Ed.*, 2010, **49**, 6058; (*b*) K. Sumida, D. L. Rogow, J. A. Mason, T. M. McDonald, E. D. Bloch, Z. R. Herm, Z. T.-H. Bae and J. R. Long, *Chem. Rev.*, 2012, **112**, 724.
3 (*a*) S. Yang, X. Lin, A. J. Blake, G. S. Walker, P. Hubberstey, N. R. Champness and M. Schröder, *Nat. Chem.*, 2009, **1**, 487; (*b*) A. J. Nuñez, L. N. Shear, N. Dahal, I. A. Ibarra, J. W. Yoon, Y. K. Hwang, J.-S. Chang and S. M. Humphrey, *Chem. Commun.*, 2011, **47**, 11855; (*c*) P. Nugent, Y. Belmabkhout, S. D. Burd, A. J. Cairns, R. Luebke, K. Forrest, T. Pham, S. Ma, B. Space, L. Wojtas, M. Eddaoudi and M. J. Zaworotko, *Nature*, 2013, **495**, 80; (*d*) K. Okada, R. Ricco, Y. Tokudome, M. J. Styles, A. J. Hill, M. Takahashi and P. Falcaro, *Adv. Funct. Mater.*, 2014, **24**, 1969; (*e*) K. Sumida, N. Moitra, J. Reboul, S. Fukumoto, K. Nakanishi, K. Kanamori, S. Furukawa and S. Kitagawa, *Chem. Sci.*, 2015, **6**, 5938.
4 (*a*) N. L. Ho, J. Perez-Pellitero, F. Porcheron and R. J.-M. Pellenq, *J. Phys. Chem. C*, 2012, **116**, 3600; (*b*) N. L. Ho, J. Perez-Pellitero, F. Porcheron and R. J.-M. Pellenq, *Langmuir*, 2011, **27**, 8187; (*c*) N. L. Ho, F. Porcheron and R. J.-M. Pellenq, *Langmuir*, 2010, **26**, 13287.
5 (*a*) A. Luzar and D. Bratko, *J. Phys. Chem. B*, 2005, **109**, 22545; (*b*) D. Bratko and A. Luzar, *Langmuir*, 2008, **24**, 1247.
6 E. Soubeyrand-Lenoir, C. Vagner, J. W. Yoon, P. Bazin, F. Ragon, Y. K. Hwang, C. Serre, J.-S. Chang and P. L. Llewellyn, *J. Am. Chem. Soc.*, 2012, **134**, 10174.
7 G. E. Cmarik, M. Kim, S. M. Cohen and K. S. Walton, *Langmuir*, 2012, **28**, 15606.
8 J. Qian, F. Jiang, D. Yuan, M. Wu, S. Zhang, L. Zhang and M. Hong, *Chem. Commun.*, 2012, **48**, 9696.
9 S. Clauzier, L. N. Ho, M. Pera-Titus, B. Coasne and D. Farrusseng, *J. Am. Chem. Soc.*, 2012, **134**, 17369.
10 G. R. Medders and F. Paesani, *J. Phys. Chem. Lett.*, 2014, **5**, 2897.
11 M. Pera-Titus, R. El-Chahal, V. Rakotovao, C. Daniel, S. Miachon and J.-A. Dalon, *ChemPhysChem*, 2009, **10**, 2082.
12 A. Zárate, R. A. Peralta, P. A. Bayliss, R. Howie, M. Sánchez-Serratos, P. Carmona-Monroy, D. Solis-Ibarra, E. González-Zamora and I. A. Ibarra, *RSC Adv.*, 2016, **6**, 9978.
13 R. Roque-Malherbe, *Microporous Mesoporous Mater.*, 2000, **41**, 227.
14 D. R. Lide, *Handbook of Chemistry and Physics*, CRC Press LLC, 84th edn, 2004.
15 J. R. Álvarez, R. A. Peralta, J. Balmaseda, E. González-Zamora and I. A. Ibarra, *Inorg. Chem. Front.*, 2015, **2**, 1080.
16 M. F. de Lange, K. J. F. M. Verouden, T. J. H. Vlugt, J. Gascon and F. Kapteijn, *Chem. Rev.*, 2015, **115**, 12205.
17 (*a*) A. L. Spek, *Acta Crystallogr., Sect. D: Biol. Crystallogr.*, 2009, **65**, 148; (*b*) A. L. Spek, *Acta Crystallogr., Sect. C: Struct. Chem.*, 2015, **71**, 9.
18 J. Duan, M. Higuchi, R. Krishna, T. Kiyonaga, Y. Tsutsumi, Y. Sato, Y. Kubota, M. Takata and S. Kitagawa, *Chem. Sci.*, 2014, **5**, 660.
19 S. Yang, J. Sun, A. J. Ramirez-Cuesta, S. K. Callear, W. I. F. David, D. P. Anderson, R. Newby, A. J. Blake, J. E. Parker, C. C. Tang and M. Schröder, *Nat. Chem.*, 2012, **4**, 887.
20 R. M. Roque-Malherbe, *Adsorption and Diffusion in Nanoporous Materials*, CRC Press, 2007.
21 D. R. Lide, *Handbook of Chemistry and Physics*, CRC Press LLC, 2004.

 This journal is © The Royal Society of Chemistry 2016